

RESEARCH ARTICLE

Climate Change and Drought Events in the Geochemical Records of the Lacustrine Deposits in the Southeastern Tibetan Plateau

Wenxiang Zhang^{1,2☯*}, Qingzhong Ming^{3☯}, Zhengtao Shi¹, Jie Niu^{1,2}, Huai Su¹

1 Key Laboratory of Geographical Process and Environmental Change in the Plateau of Yunnan Province, Kunming, China, **2** Key Laboratory of Plateau Lake Ecology and Global Change, Yunnan Normal University, Kunming, China, Yunnan University of Finance and Economics, Kunming, China, **3** Yunnan University of Finance and Economics, Kunming, China

☯ These authors contributed equally to this work.

* wenxiangzhang@gmail.com



OPEN ACCESS

Citation: Zhang W, Ming Q, Shi Z, Niu J, Su H (2016) Climate Change and Drought Events in the Geochemical Records of the Lacustrine Deposits in the Southeastern Tibetan Plateau. PLoS ONE 11 (12): e0168928. doi:10.1371/journal.pone.0168928

Editor: Liping Zhu, Institute of Tibetan Plateau Research Chinese Academy of Sciences, CHINA

Received: July 13, 2016

Accepted: December 8, 2016

Published: December 29, 2016

Copyright: © 2016 Zhang et al. This is an open access article distributed under the terms of the [Creative Commons Attribution License](https://creativecommons.org/licenses/by/4.0/), which permits unrestricted use, distribution, and reproduction in any medium, provided the original author and source are credited.

Data Availability Statement: All relevant data are within the paper.

Funding: This study was supported by the Cultivating Talents of the Middle-aged Academic and Technology Leaders of Yunnan Province (No. 2015HB029), the Open Fund of State Key Laboratory of Loess and Quaternary Geology (SKLLQG1020) and the National Natural Science Foundation of China (No. U0933604).

Competing Interests: The authors have declared that no competing interests exist.

Abstract

Lacustrine deposits at the margin of the southeastern Tibetan Plateau (SETP) are sensitive indicators for the evolution of the southwest Asian monsoon (SWAM) during the Quaternary. Thus, they can provide insight into the Quaternary climatic history and their relationship with global climatic changes. The results of the geochemical analysis of the Xiaozhongdian Basin section at the SETP suggest that SiO₂ had the highest content of the major elements followed by Al₂O₃. The order of the abundance of the major elements was generally as follows: SiO₂>Al₂O₃>Fe₂O₃>CaO>MgO>K₂O>TiO₂>Na₂O>MnO₂. The geochemical proxies, such as chemical index of alteration (CIA), the index of compositional variability (ICV) and (CaO+K₂O+Na₂O)/Al₂O₃, indicate the weak chemical weathering and the aridification of the margin of the SETP during the Heinrich events. In addition, the aridification of the SETP during the Heinrich events may be closely related to the cold signals transmitted from the high latitudes of the North Atlantic to the TP, and the effect caused the cooling effect to be very strong on the TP as a result of the upper-level westerly jet stream and then reduced the suction action associated with the SWAM, thus accelerating the drying rate of Xiaozhongdian Basin, which was amplifying the degree of drought in Heinrich events.

Introduction

Geochemical elements are useful indicators of chemical weathering, geological processes and tectonic settings of sedimentary catchments. They can also be used to reconstruct the catchment paleoclimatic and environmental changes [1–3]. Studying the chemical proxies of elements in lacustrine sediments allows us to understand the close interdependence of the Asian monsoon evolution and the global climate changes [4–11]. The Tibetan Plateau (TP) has always been the object of intense climate research [12, 13]. Previous research suggests that the TP is one of the regulators of global climate [14, 15]. The Xiaozhongdian Basin (XB) is located at the margin of the southeastern TP (SETP), the climate is obviously controlled by the Asian

southwest monsoon and local climatic influences of the Qinghai-Tibet Plateau. Recent studies have found that historical records and reconstructions showed that variability in summer monsoon precipitation led to droughts [16–18]. And three Quaternary lacustrine deposition cycles and five sand layers have been identified in the XB [19]. Therefore, it is important to provide high-resolution and typically abundant environmental and climatic information to study the impact of the TP on the climatic events of the southwest Asian monsoon (SWAM) region, and it is critical to be able to evaluate the influence of global change on regional climate.

We aim to establish the geochemical weathering processes in the XB and evaluate the coupling mechanism between the Dansgaard-Oeschger records of the XB and the TP based on the high-resolution geochemical proxy analysis of XB lacustrine deposits.

Study Area

The XB is located in the Hengduan Mountains of the SETP and approximately 80 km northwest of Yulong Mountain (Fig 1). The XB is a Cenozoic faulted depression and it is controlled by the SWAM [20, 21]. Many cycles of lacustrine deposition have occurred in the XB and the total thickness of the deposits in the basin is approximately 100 m over an area of 400 km². The extremely thick lacustrine deposits in the basin have recorded the regional environmental and climatic changes over time; therefore, the XB is an ideal area for studying the evolution of the southwest monsoon. The mean annual temperature for the basin based on data recorded at regional weather stations is approximately 5.8°C and the mean annual precipitation is approximately 850 mm, with more than 85% of the precipitation occurring between June and September [22].

Sampling and Methods

Stratigraphy and sampling

A 15.3-m section along the Jinsha River (27°36'54"N, 99°45'45"E, ~3300 m asl) was excavated in the XB to obtain samples (Fig 1). The top of the section is developed recent soil with massive texture, aggregated structure and abundant plant roots from a depth of 0 to 0.4 m. The section is light grayish green in color and it is mainly composed of silty clay. There are five coarse silt layers in the middle of the section, with thicknesses of 1.7–2.2 m, 3.2–3.5 m, 7–7.2 m, 11.8–12.2 m and 14.2–14.3 m, respectively. The layer between 14.7 and 15.2 m is black clay with enriched carbon. A total of 62 samples were collected from the section at depth intervals of 25 cm for analysis of the geochemical elements. No specific permissions are required for our study locations and sampling activities.

Analytical methods

The carbonates in the samples were removed from the samples using 1 mol/L HCl before the analysis and were repeated twice. All subsamples consisting of 4 g of each sample (<75 μm) were pressurized with boric acid to 30 t/m² for 20 s. The elemental analysis of the samples was performed using a Philips PW2403 X-ray fluorescence (XRF) spectroscope. The analyzed oxide compounds are identified in elemental form in the Results and Discussion section below. Repeated analyses were performed for every 10 samples to verify the reliability and accuracy of the analytical data. The method has been used to the analysis of standard samples (lake sediment of the national soil standard reference material, GSS-9) with relative standard deviation (RSD) less than 2%.

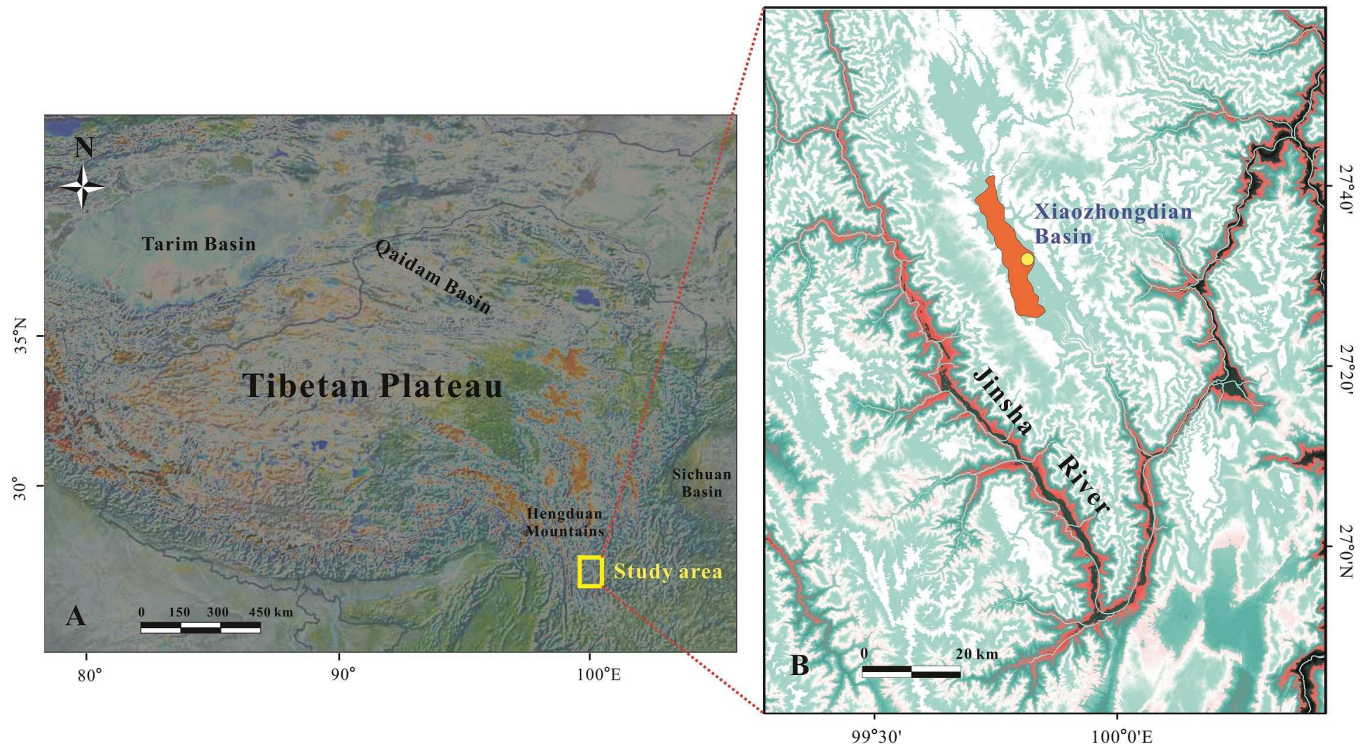


Fig 1. The location and digital elevation model of the Xiaozhongdian Basin lacustrine deposits (the data come from <http://srtm.csi.cgiar.org> for open-source. The figure is similar but not identical to the original image of SRTM, and is therefore for illustrative purposes only.)

doi:10.1371/journal.pone.0168928.g001

Seven plant macrofossil samples were collected from the organic-rich horizons of the sediment, and were used to perform ^{14}C dating. The ^{14}C dates were calibrated to calendar years by the latest calibration program [23]. The XRF analyses and ^{14}C dating were performed at the Key Laboratory of Western China’s Environmental System of Ministry of Education in Lanzhou University.

Results and Discussion

Age model and chronology

The measured dates of the study section are presented in Table 1. The ages and the records of the environmental proxies indicate there was continuous sedimentation that extended back to ~42.6 cal ka BP based on the Bayesian model of age-depth (Fig 2). The sedimentation rate in the section is approximately and 0.385 and 0.461 mm/a. The estimated sedimentation rate

Table 1. Radiocarbon dating of the lake sediment of Xiaozhongdian Basin and the age model.

Depth (m)	Dating material	AMS ^{14}C age (^{14}C yr BP)	Calibrated ^{14}C (2σ , cal a BP)
1.7	Plant remains	9390–9650	10503–11203
3.9	Plant remains	14505–14915	17425–18421
5.2	Plant remains	16420–16980	19573–20343
7.5	Plant remains	19880–20580	23673–24617
9.4	Plant remains	23380–24370	28215–29360
12.2	Plant remains	25560–26820	30464–31562
14.7	Plant remains	30250–33970	38215–41993

doi:10.1371/journal.pone.0168928.t001

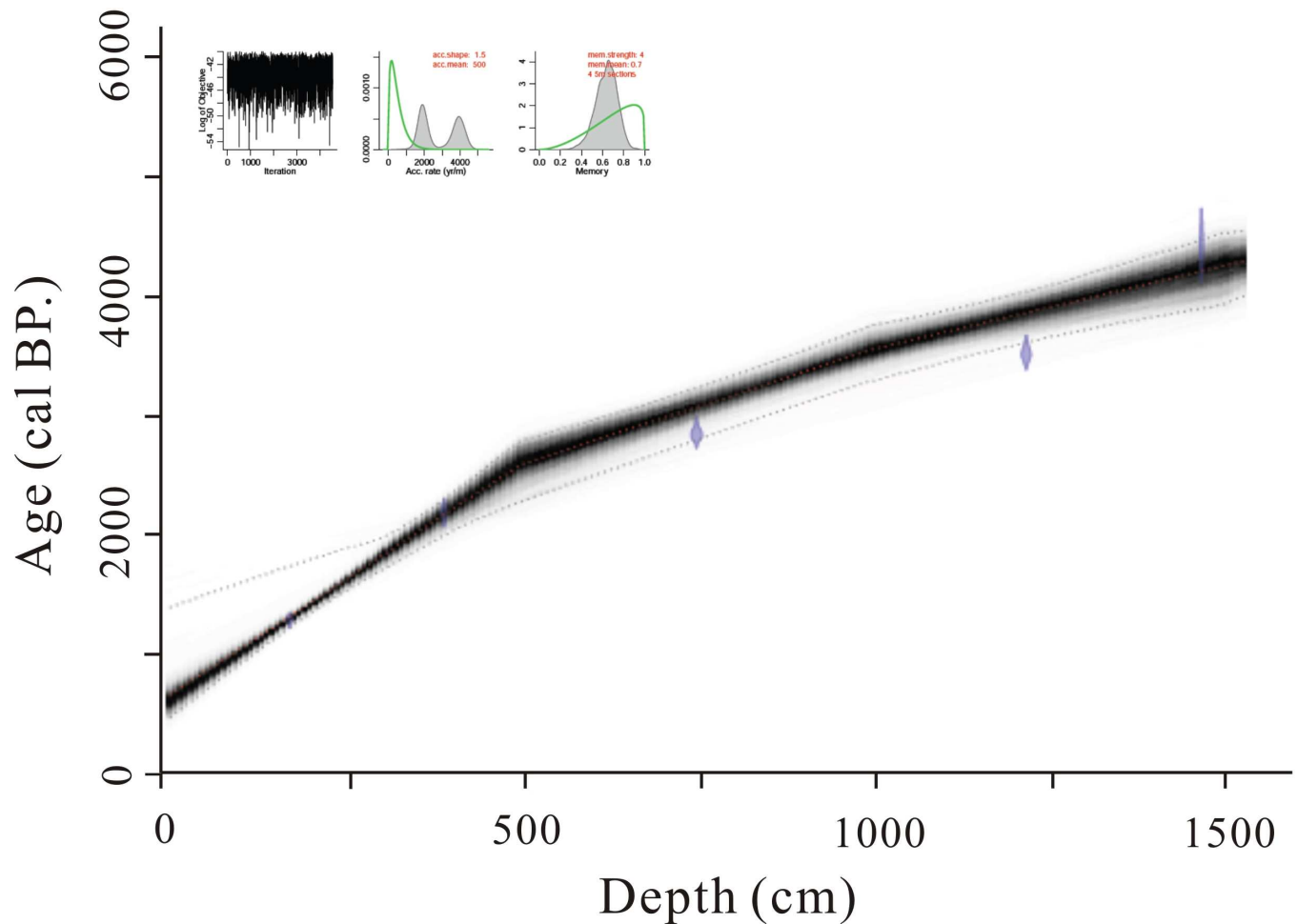


Fig 2. The Bayesian age-depth model of the Xiaozhongdian Basin section.

doi:10.1371/journal.pone.0168928.g002

corresponds with other geochronology in Yunnan Province [24, 25]. The characteristics of chemical weathering and climate change in the layer (1.75–0 m) of XB section were not included in the following analyses because it has the only ^{14}C data around the Holocene.

Geochemical element characteristics

The compositions of SiO_2 , Al_2O_3 , Fe_2O_3 , CaO , MgO , K_2O , TiO_2 , Na_2O and MnO_2 are shown in Fig 3. The total oxide content of the samples ranges from 90.56% to 93.15%, with an average value of 91.76%. SiO_2 has the highest content of all the analyzed major elements and ranges from 53.51% to 65.40%, with an average value of 57.23%, followed by Al_2O_3 , with an average content of 14.09%. The regularity of the abundance of oxide compounds in the XB section was as follows: $\text{SiO}_2 > \text{Al}_2\text{O}_3 > \text{Fe}_2\text{O}_3 > \text{CaO} > \text{MgO} > \text{K}_2\text{O} > \text{TiO}_2 > \text{Na}_2\text{O} > \text{MnO}_2$. In addition, the content of each element indicated substantial fluctuations for the five sand layers, especially the element Ti, which is generally recognized as being mainly derived from the lake sediments.

Geochemical proxies and paleoclimatic significance

The characteristics of the geochemical proxies not only indicate the degree of chemical weathering in the lake catchment, but can also indicate the conditions of climate evolution and the

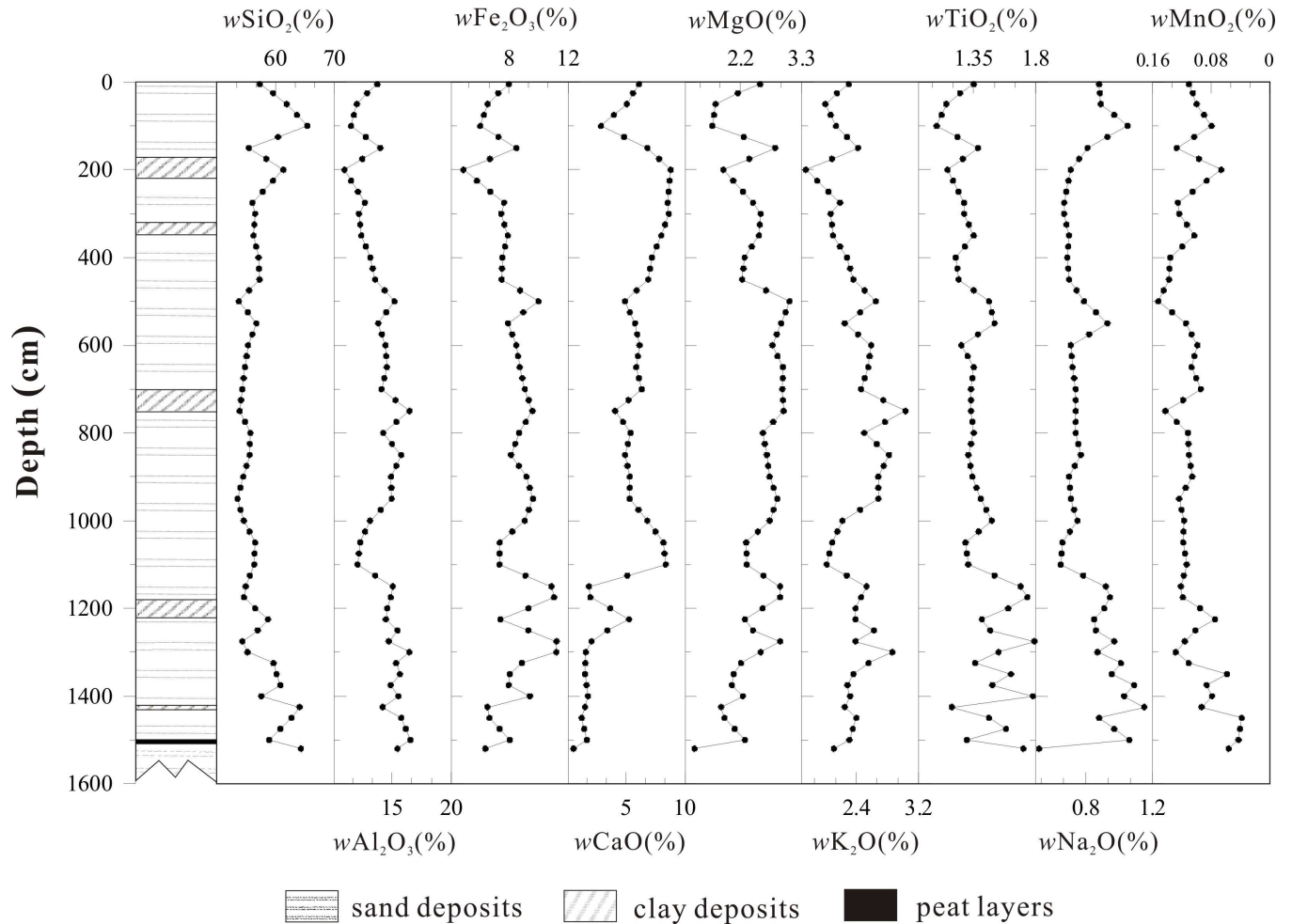


Fig 3. Variation of oxide and element contents in the Xiaozhongdian Basin section.

doi:10.1371/journal.pone.0168928.g003

changes in the depositional environment [26–28]. Therefore, the geochemical elements of lacustrine deposits can be used to study climate change [29, 30]. The values of $(CaO+K_2O+Na_2O)/Al_2O_3$, the index of mineral chemical differentiation (ICV) and the chemical weathering index (CIA) can represent paleoclimatic proxies of the chemical weathering intensity and effective moisture [31, 32].

The chemical index of alteration (CIA): The CIA is one of the measures indexes for studying the intensity of chemical weathering [33–35]:

$$CIA = Al_2O_3 / (Al_2O_3 + K_2O + Na_2O + CaO^*) \times 100 \quad (1)$$

where the oxide amounts are expressed in moles, and CaO^* is the amount of CaO in silicates [36–38]. The effect of carbonate minerals has been ruled out in CIA, which mainly reflects the weathering intensity of silicate minerals, so it can well reflect the chemical weathering of the source area. Previous studies have shown that the warm-humid climate and environment would cause to increase the chemical weathering and further analyze the climate of lake catchment by using CIA [29]. The chemical weathering proxies (e.g. CIA, ICV) have been applied to the study of the climate of lake catchment [30–32]. In general, the warm-humid climate and environment would cause to increase the chemical weathering, and CIA values

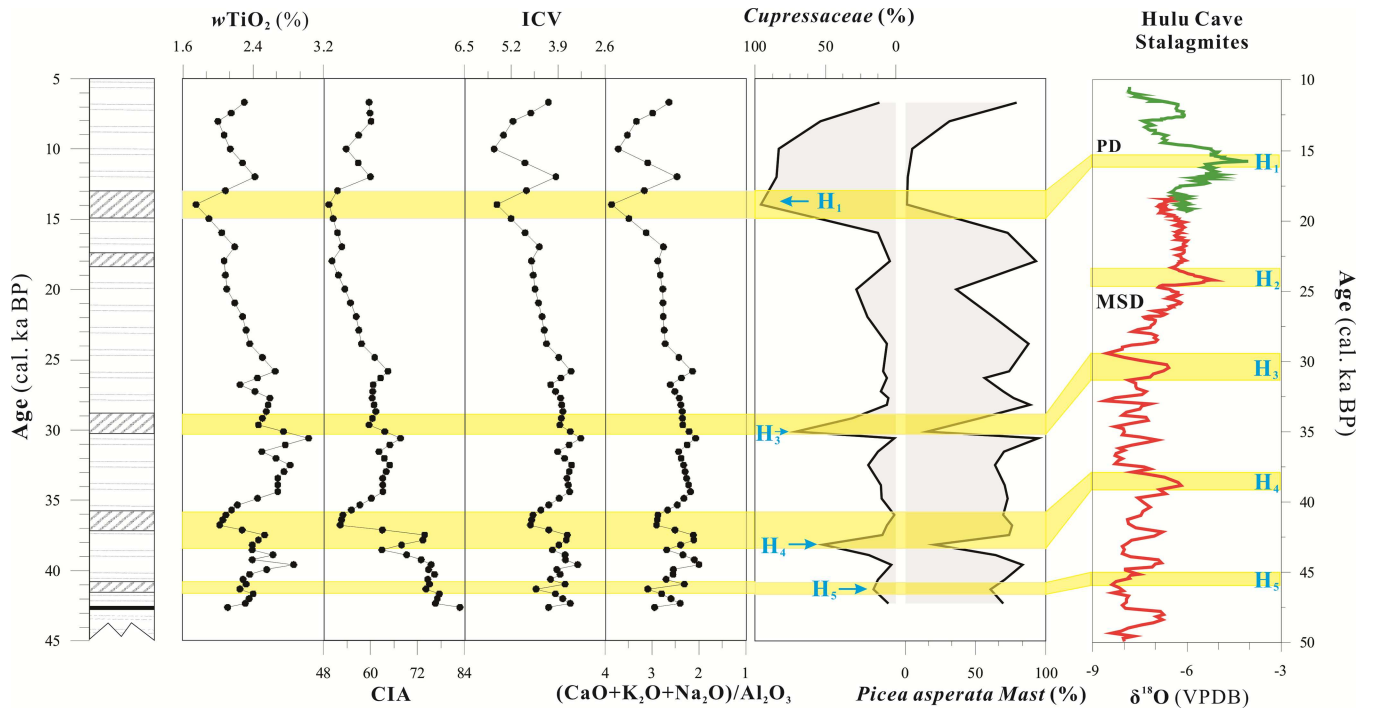


Fig 4. The characteristics of geochemical proxy, sporopollen in the Xiaozhongdian Basin and $\delta^{18}\text{O}$ of Hulu Cave stalagmites [39] (the abundance data for *Cupressaceae* and *Picea asperata Mast* is from [19]).

doi:10.1371/journal.pone.0168928.g004

ranging from 70 to 85 indicate the intense chemical weathering and a warm and humid climate. The main source of the lacustrine sediments in Xiaozhongdian paleolake mainly came from the Basin, and it was relatively simple [20]. Therefore, CIA can be seen as the proxy to study the chemical weathering, climatic and environmental change of lake catchment in XB. The CIA of the XB section ranged from 49.37 to 82.90, the major distribution range between 50 and 70, which is the same as the range of CIA values for basalt and average shale throughout the world (Figs 4 and 5), showed that the climatic conditions were weak chemical weathering,

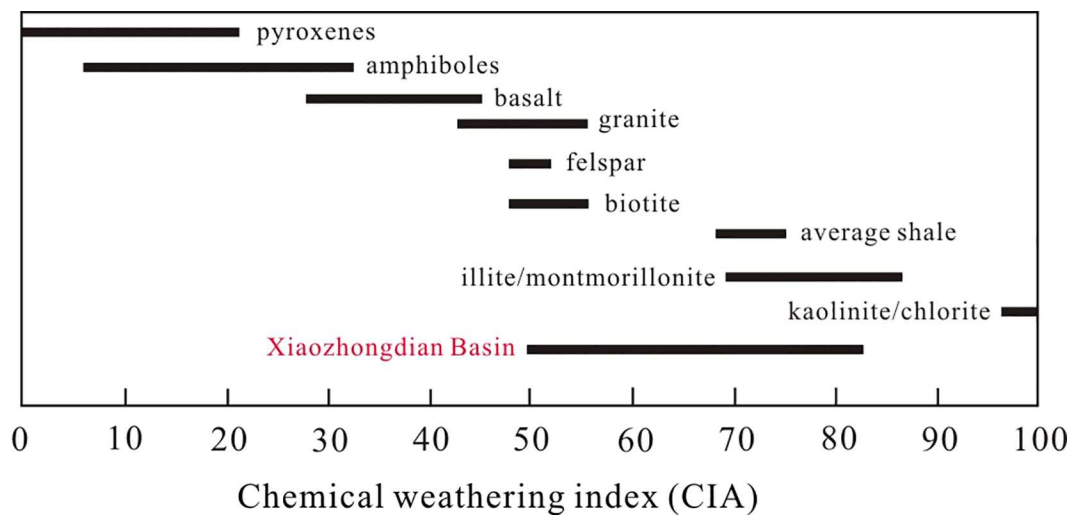


Fig 5. Comparison of CIA for Xiaozhongdian Basin sediments with CIAs for rock and minerals (Based on [33, 34]).

doi:10.1371/journal.pone.0168928.g005

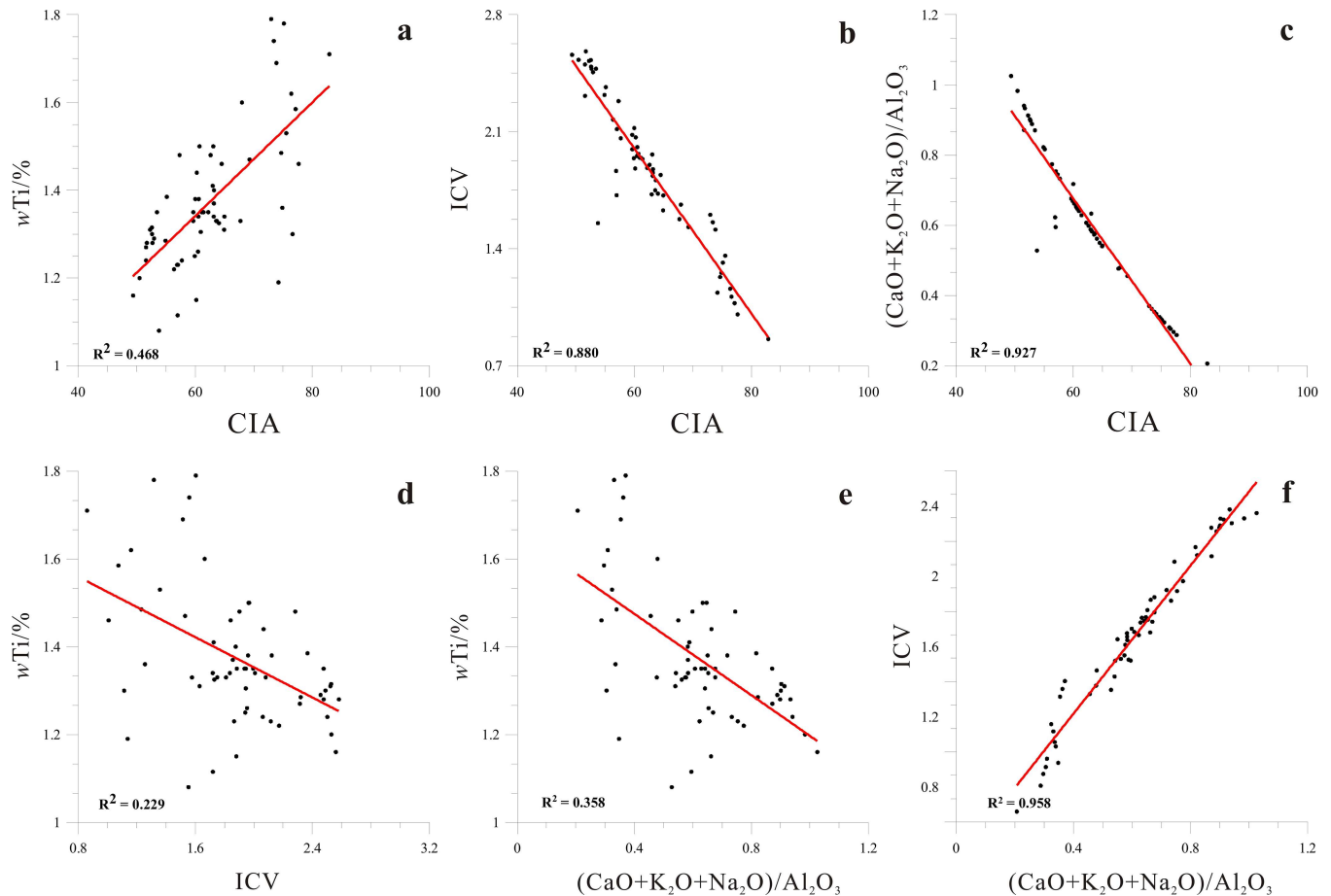


Fig 6. The correlation among the TiO₂ contents, CIA, ICV and (CaO+K₂O+Na₂O)/Al₂O₃.

doi:10.1371/journal.pone.0168928.g006

and it also indicated the relatively the cold-dry climate, except for the period of 42.6–36.8 cal ka BP (15.2–11.5 m). The CIA varies from 49.4 to 67.7 for the time period of 37.4–11.0 cal ka BP (11.5–1.25 m), with an average value of 58.6, which slightly exceeds the CIA value for feldspar, it indicated the weak chemical weathering and dry climate of the lake catchment. The results of correlation analyses of the proxies indicated a good correlation between the CIA and the content of the element Ti, with $R^2 = 0.468$ ($P < 0.01$, Fig 6A).

The index of compositional variability (ICV): Elements preferentially leach and migrate under the warm and humid climate conditions. However, it is difficult for the element Al to migrate during the chemical weathering. Therefore, the ICV can be used to study the proportion of active components in lacustrine deposits. The ICV is expressed as [40]:

$$ICV = (Fe_2O_3 + K_2O + Na_2O + CaO + MgO + MnO + TiO_2) / Al_2O_3 \quad (2)$$

The different minerals have different ICV intervals, the ICV of non-clay minerals is higher than that of clay minerals, and the ICV of pyroxene is between 10 and 100. The ICV values for amphibole, K feldspar, plagioclase, and illite/muscovite are 8, 1, 0.6 and 0.3, respectively, and the range of CIV values for montmorillonite and kaolinite are only 0.15–0.3 and 0.03–0.05, respectively. The high ICV value indicates the intensity of chemical weathering, and reflects the optimal hydrothermal quality for the climatic conditions of the XB [41]. The ICV of the

XB ranges from 0.86 to 2.58, with an average of 1.87 (Fig 4), and it is substantially higher than the ICV values of feldspar and clay minerals. The ICV values of XB show an increasing trend from the bottom to the top of the section. The results of the correlation analyses of the proxies indicated good correlations between ICV and Ti and between ICV and CIA, with $R^2 = 0.229$ and 0.880, respectively ($P < 0.01$, Fig 6B and 6D). The good correlations indicate the weak chemical weathering and the poor hydrothermal quality of the climatic conditions of the XB at the margin of the SETP.

$(CaO+K_2O+Na_2O)/Al_2O_3$: The geochemical behavior of active chemical elements, such as Na, Ca, K, has been affected by climate change during hypergenesis [42]. Aluminum silicate is often changed into clay minerals (e.g. illite, montmorillonite and kaolinite) as a result of chemical weathering. In extremely hot and humid climatic conditions, the clay minerals are decomposed and form bauxite. Therefore, the value of $(CaO+K_2O+Na_2O)/Al_2O_3$ in the paleolake in the XB reflect the relationship between the active and inert components and record the change in the climatic conditions. A high value of $(CaO+K_2O+Na_2O)/Al_2O_3$ for the lake sediment demonstrate the weak weathering and the low effective moisture dominating the environment and climate. The $(CaO+K_2O+Na_2O)/Al_2O_3$ for most of the samples indicates a range from 0.21 to 1.03, with an average value of 0.62 (Fig 4). There are good correlations between $(CaO+K_2O+Na_2O)/Al_2O_3$ and Ti, $(CaO+K_2O+Na_2O)/Al_2O_3$ and CIA, and $(CaO+K_2O+Na_2O)/Al_2O_3$ and ICV ($P < 0.01$, Fig 6C, 6E and 6F). The good correlations demonstrate the weak leaching movement of elements in the section, the low effective moisture and the dry climate of the XB in the Heinrich (H) events.

Climate evolution and driving mechanism in the SETP

The chemical weathering process and the history of environmental change of the XB between 42.6 and 11 ka cal. BP were reconstructed based on the geochemical characteristics and other climate proxies combined with the regional research [22, 43]. The coarse silt layers in the middle of the section records the multiple extreme climate events of XB, and eventually lead to the disappearance of Xiaozhongdian paleolake. The records of Heinrich events in the lacustrine deposits are particularly noticeable in the section. Previous studies have shown that the records of Heinrich events were difference in the world. The records of Heinrich events were represented as drought in the Bay of Bengal region and India [44, 45]. In the East Asian monsoon region, it appeared as cold and dry [46–49]. However, it indicated the humid climate in South American and the Australian [50, 51]. At the same time, the latest research shows that the signal of stalagmite isotope in China has reflected the dry/wet process under the controlling of monsoon climate [52]. Fig 4 compares the distribution patterns between the geochemical records of the lacustrine deposits and $\delta^{18}O$ of Hulu Cave stalagmite [39]. By comparison, Heinrich events were recorded relatively well in the geochemical and sporopollen records of XB and $\delta^{18}O$ of Hulu Cave stalagmite, except H₂ event. The records of H₁, H₃, H₄ events are relatively more remarkable, and that of H₅ less obvious. In general, the instabilities of the climatic characteristics of the SWAM are mainly affected by the interaction among ice sheets, the ocean and the atmosphere and the climate signals of high latitudes passing to low latitudes through thermohaline circulation [53]. The TP can be regarded as a regulator that enlarged or reduced the signals during the H events in the SETP [54]. During the H events, the cold signals were transmitted from the high latitudes of the North Atlantic to the TP. In turn, this effect caused the cooling effect to be very strong on the TP as a result of the upper-level westerly jet stream and then reduced the suction action associated with the SWAM [55], thus accelerated the drying rate of Xiaozhongdian Basin, which was amplifying the degree of drought in Heinrich events.

Conclusions

The geochemical characteristics and their parameters for the Xiaozhongdian Basin lacustrine deposits recorded the millennial scale history of the SWAM evolution and a series of the drought events corresponding to the Heinrich events.

By comparing research conducted in the study region and other regions, the TP can be considered a climate regulator that enlarged or reduced the signals associated with the suction action during the H and D/O events. The forms of the climatic events in the various regions of China are related to the effect of the suction action of the TP. The record of the Heinrich events of the SETP indicated more substantial drought events. The warmer climate further increased the evaporation of the study area, which was amplifying the degree of drought. However, the regional records for other regions of China have indicated rapid cooling because of the less pronounced effect by the TP. It would be beneficial to explore the regional climate characteristics and their relationships with the global patterns.

Acknowledgments

We are grateful to Jixiu Cao, the key laboratory of western china's environmental systems of MOE, for his assistance during the laboratory work. We thank Shupeng Gao (School of Tourism and Geographical Sciences, Yunnan Normal University) for helping to make mapping. Special thanks the academic editor Prof. Liping Zhu and the anonymous reviewers for comments that greatly improve the manuscript.

Author Contributions

Conceptualization: QM.

Formal analysis: WZ QM ZS HS.

Funding acquisition: WZ QM.

Investigation: QM ZS.

Methodology: WZ QM HS.

Software: WZ JN.

Writing – original draft: WZ HS.

Writing – review & editing: WZ QM JN.

References

1. Taylor SR, McLennan SM. *The Continental Crust: its Composition and Evolution*. London: Blackwell scientific publications. 1985.
2. Zhang HC, Zhang WX, Chang FQ, Yang LQ, Lei GL, Yang MS, et al. Geochemical fractionation of rare earth elements in lacustrine deposits from Qaidam Basin. *Science in China* 2009; 52: 1703–1713.
3. Li MH, Zhu LP, Wang JB, Wang LQ, Yi CL, Galy A. Multiple implications of rare earth elements for Holocene environmental changes in Nam Co, Tibet. *Quaternary International* 2011; 236: 96–106.
4. Overpeck J, Anderson D, Trumbore S, Prell W. The southwest Indian Monsoon over the last 18,000 years. *Climate Dynamics* 1996; 12(3): 213–225.
5. Sahai AK, Grimm AM, Satyan V, Pant GB. Long-lead prediction of Indian summer monsoon rainfall from global SST evolution. *Climate Dynamics* 2003; 20(7–8): 855–863.
6. Tarasov P, Granoszewski W, Bezrukova E, Brewer S, Nita M, Abzaeva A, et al. Quantitative reconstruction of the last interglacial vegetation and climate based on the pollen record from Lake Baikal, Russia. *Climate Dynamics* 2005; 25(6): 625–637.

7. Wang PX, Clemens S, Beaufort L, Braconnot P, Ganssen G, Jian Z, et al. Evolution and variability of the Asian monsoon system: state of the art and outstanding issues. *Quaternary Science Reviews* 2006; 24(5–6): 595–629.
8. Vogel H, Wagner B, Zanchetta G, Sulpizio R, Rosén P. A paleoclimate record with tephrochronological age control for the last glacial-interglacial cycle from Lake Ohrid, Albania and Macedonia. *Journal of Paleolimnology* 2010; 44(1): 295–310.
9. Bartlein PJ, Harrison SP, Brewer S, Connor S, Davis BAS, Gajewski K, et al. Pollen-based continental climate reconstructions at 6 and 21 ka: a global synthesis. *Climate Dynamics* 2011; 37(3–4): 775–802.
10. Xu H, Hong Y, Hong B. Decreasing Asian summer monsoon intensity after 1860 AD in the global warming epoch. *Climate Dynamics* 2012; 39(7–8): 2079–2088.
11. Zhang WX, Shi ZT, Chen GJ, Liu Y, Niu J, Ming QZ, et al. Geochemical characteristics and environmental significance of Taledo loess-paleosol sequences of Ili Basin in Central Asia. *Environmental Earth Sciences* 2013; 70(5): 2191–2202.
12. Clark MK, Schoenbohm LM, Royden LH, Whipple KX, Burchfiel BC, Zhang X, et al. Surface uplift, tectonics, and erosion of eastern Tibet from large-scale drainage patterns. *Tectonics* 2004; 23(1): 241–262.
13. Zhu LP, Lü XM, Wang JB, Peng P, Kasper T, Daut G, et al. Climate change on the Tibetan Plateau in response to shifting atmospheric circulation since the LGM. *Scientific Reports* 2015; 5: 13318. doi: [10.1038/srep13318](https://doi.org/10.1038/srep13318) PMID: [26294226](https://pubmed.ncbi.nlm.nih.gov/26294226/)
14. Li J, Fang X. Uplift of the Tibetan Plateau and environmental changes. *Chinese Science Bulletin* 1999; 44(23): 2117–2124.
15. Kong P, Zheng Y, Caffee MW. Provenance and time constraints on the formation of the first bend of the Yangtze River. *Geochemistry Geophysics Geosystems* 2012; 13(6): 96–109.
16. Cook ER, Anchukaitis KJ, Buckley BM, D'Arrigo RD, Jacoby GC, Wright WE. Asian monsoon failure and megadrought during the last millennium. *Science* 2010; 328: 486–489. doi: [10.1126/science.1185188](https://doi.org/10.1126/science.1185188) PMID: [20413498](https://pubmed.ncbi.nlm.nih.gov/20413498/)
17. Ponton C, Giosan L, Eglinton TI, Fuller DQ, Johnson JE, Kumar P, et al. Holocene aridification of India. *Geophysical Research Letters* 2012; 39(3): L03704.
18. Sinha A, Stott L, Berkelhammer M, Cheng H, Edwards RL, Buckley B, et al. A global context for megadroughts in monsoon Asia during the past millennium. *Quaternary Science Review* 2011; 30: 47–62.
19. Ming QZ, Su H, Shi ZT, Dong M, Zhang WX. Last Five Heinrich Events Revealed by Lacustrine Sediments from Xiaozhongdian Basin in Yunnan Province. *Acta Geographica Sinica* 2011; 66(1): 123–130.
20. Zhao XT, Zheng MP, Li DM. Formation and Evolution of the Ancient "Lake Xiaozhongdian" in Diqing, Yunnan and Its Relationship with Development of the Ancient "Lake Shigu" and the Modern Valley of the Jinsha River. *Acta Geologica Sinica* 2007; 81(12): 1645–1651.
21. Xu H, Sheng E, Lan J, Liu B, Yu K, Che S, et al. Decadal/multi-decadal temperature discrepancies along the eastern margin of the Tibetan Plateau. *Quaternary Science Reviews* 2014; 89: 85–93.
22. Yin Y, Fang NQ, Sheng JF, Hu CY, Nie HG. Lacustrine records of environmental changes during the last 57 ka in the Napahai lake, northwestern Yunnan, China. *Marine Geology & Quaternary Geology* 2002; 22(4): 99–105.
23. Reimer PJ, Bard E, Bayliss A, Beck JW, Blackwell PG, Ramsey CB, et al. IntCal13 and Marine13 radiocarbon age calibration curves 0–50,000 years cal BP. *Radiocarbon* 2013; 55(4): 1869–1887.
24. Hodell DA, Brenner M, Kanfoush SL, Curtis JH, Stoner JS, Song X, et al. Paleoclimate of southwestern China for the past 50,000 yr. inferred from lake sediment records. *Quaternary Research*. 1999; 52: 369–380.
25. Zhang WX, Ming QZ, Shi ZT, Chen GJ, Niu J, Lei GL, et al. Lake sediment records on climate change and human activities in the Xingyun Lake catchment, SW China. *Plos One* 2014; 9(3): e02167.
26. McLennan S M. Weathering and global denudation. *Journal of Geology*. 1993; 101: 295–303.
27. Liu L, Wang H, Chen J. Reconstruction of the rainfall on the Chinese Loess Plateau during the past 130 ka from the dolomite distributions. *Geochim Cosmochim Acta* 2006; 70: 363.
28. Li Y, Wang N, Cheng HY, Long H, Zhao Q. Holocene environmental change in the marginal area of the Asian monsoon: a record from Zhuye Lake, NW China. *Boreas* 2009; 38(2): 349–361.
29. Roy PD, Caballero M, Lozano S, Morton O, Lozano R, Jonathan MP, et al. Provenance of sediments deposited at paleolake San Felipe, western Sonora Desert: Implications to regimes of summer and winter precipitation during last 50 cal kyr BP. *Journal of Arid Environments* 2012; 81: 47–58.
30. Park J, Lim HS, Lim J, Park YH. High-resolution multi-proxy evidence for millennial- and centennial-scale climate oscillations during the last deglaciation in Jeju Island, South Korea. *Quaternary Science Reviews* 2014; 105: 112–125.

31. Lee MK, Lee YI, Lim HS, Lee JI, Yoon HI. Late Pleistocene-Holocene records from Lake Ulaan, southern Mongolia: implications for east Asian palaeomonsoonal climate changes. *Journal of Quaternary Science* 2013; 28(4): 370–378.
32. Wu YH, Li SJ, Xia WL. Element geochemistry of lake sediment from Gourenco lake, Kekexili, Qinghai-Xizang plateau and its significance for climate variation. *Journal of Earth Science & Environmental* 2004; 26: 64–68.
33. Nesbitt HW, Young GM, McLennan SM, Keays RR. Effects of Chemical Weathering and Sorting on the Petrogenesis of Siliciclastic Sediments, with Implications for Provenance Studies. *Journal of Geology* 1996; 104(5): 525–542.
34. Young GM. Geochemical investigation of a Neoproterozoic glacial unit: the mineral fork formation in the Wasatch Range. Utah. *GSA Bull* 2002; 114: 387–399.
35. Wei ZQ, Zhong W, Chen YQ, Tan LL. Supergene geochemical elements of swampy basin in the subtropical monsoon region: a case study of Dingnan Dahu in Jiangxi Province. *Progress in Geography* 2015, 34: 909–917.
36. Nesbitt HW, Markovics G, Price RC. Chemical processes affecting alkalis and alkaline earths during continental weathering. *Geochim Cosmochim Acta* 1980; 44: 1659–1666.
37. Nesbitt HW, Young GM. Early Proterozoic climates and plate motions inferred from major element chemistry of lutites. *Nature* 1982; 299: 715–717.
38. Gallet S, Jahn BM, Lanoë BVV, Dia A, Rossello E. Loess geochemistry and its implications for particle origin and composition of the upper continental crust. *Earth & Planetary Science Letters* 1998; 156(3–4): 157–172.
39. Wang YJ, Cheng H, Edwards RL, An ZS, Wu JY, Shen CC, et al. A high-resolution absolute-dated late Pleistocene Monsoon record from Hulu Cave, China. *Science* 2002; 294(5550): 2345–2348.
40. Cox R. The influence of sediment recycling and basement composition on evolution of mudrock chemistry in the southwestern United States. *Geochimica et Cosmochimica Acta* 1995; 59: 2919–2940.
41. Joo YJ, Lee YI, Bai Z. Provenance of the Qingshuijian Formation (Late Carboniferous), NE China: Implications for tectonic processes in the northern margin of the North China block. *Sedimentary Geology* 2005; 177(1): 97–114.
42. Zhang WX, Zhang HC, Lei GL, Yang LQ, Niu J, Chang FQ, et al. Elemental geochemistry and paleoenvironment evolution of Shell Bar section at Qarhan in the Qaidam Basin. *Quaternary Sciences* 2008; 28: 917–928.
43. An ZS, Clemens SC, Shen J, Qiang XK, Jin ZD, Sun YB, et al. Glacial-interglacial indian summer monsoon dynamics. *Science* 2011; 333: 719–23. doi: [10.1126/science.1203752](https://doi.org/10.1126/science.1203752) PMID: [21817044](https://pubmed.ncbi.nlm.nih.gov/21817044/)
44. Peterson LC, Haug GH, Hughen KA, Röhl U. Rapid changes in the hydrologic cycle of the tropical Atlantic during the last glacial. *Science* 2000; 290: 1947–1951. PMID: [11110658](https://pubmed.ncbi.nlm.nih.gov/11110658/)
45. Stott L, Poulsen C, Lund S. Super ENSO and global climate oscillations at millennial time scales. *Science* 2002; 297: 222. doi: [10.1126/science.1071627](https://doi.org/10.1126/science.1071627) PMID: [12114618](https://pubmed.ncbi.nlm.nih.gov/12114618/)
46. Yuan DX, Cheng H, Lawrence ER, Dykoski CA, Kelly MJ, Zhang M, et al. Timing, Duration, and Transitions of the Last Interglacial Asian Monsoon. *Science* 2004; 304(5670): 575–578. doi: [10.1126/science.1091220](https://doi.org/10.1126/science.1091220) PMID: [15105497](https://pubmed.ncbi.nlm.nih.gov/15105497/)
47. Dykoski CA, Edwards RL, Cheng H, Yuan DX, Cai YJ, Zhang M, et al. A high-resolution, absolute-dated Holocene and deglacial Asian monsoon record from Dongge Cave, China. *Earth & Planetary Science Letters* 2005; 233(s 1–2): 71–86.
48. Wang YJ, Cheng H, Edwards RL, Kong XG, Shao XH, Chen ST, et al. Millennial- and orbital-scale changes in the East Asian monsoon over the past 224,000 years. *Nature* 2008; 451(7182): 1090–1093. doi: [10.1038/nature06692](https://doi.org/10.1038/nature06692) PMID: [18305541](https://pubmed.ncbi.nlm.nih.gov/18305541/)
49. Zhou H, Zhao JX, Feng Y, Chen Q, Mi X, Shen CC, et al. Heinrich event 4 and Dansgaard/Oeschger events 5–10 recorded by high-resolution speleothem oxygen isotope data from central China. *Quaternary Research* 2014; 82(2): 394–404.
50. Leuschner DC, Sirocko F. The low-latitude monsoon climate during Dansgaard-Oeschger cycles and Heinrich events. *Quaternary Science Reviews* 2000; 19(1–5): 243–254.
51. Muller J, Kylander M, Wüst RAJ, Weiss D, Martinez-Cortizas A, Legrande AN, et al. Possible evidence for wet Heinrich phases in tropical NE Australia: The Lynch's Crater deposit. *Quaternary Science Reviews* 2008; 27(5–6): 468–475.
52. Wang YJ, Liu DB. Speleothem records of Asian paleomonsoon variability and mechanisms. *Chinese Science Bulletin* 2016; 61: 938–951.
53. Rahmstorf S. Rapid climate transitions in a coupled ocean-atmosphere model. *Nature* 1994; 372: 82–85.

54. Fang XM, Lü LQ, Mason JA, Yang SL, An ZS, Li J, et al. Pedogenic response to millennial summer monsoon enhancements on the Tibetan Plateau. *Quaternary International* 2003; 2(106–107): 79–88.
55. Weber ME, Wiedicke-Hombach M, Kudrass HR, Erlenkeuser H. Bengal Fan sediment transport activity and response to climate forcing inferred from sediment physical properties. *Sedimentary Geology* 2003; 155(3–4): 361–381.